International Journal of Engineering and Technical Research (IJETR)
ISSN: 2321-0869 (O) 2454-4698 (P), Volume-7, Issue-8, August 2017

Modeling of ionic transport through nanofiltration membranes considering zeta potential and dielectric exclusion phenomena

Marcela Costa Ferreira, João Victor Nicolini, Heloísa L. S. Fernandes, Fabiana Valéria da Fonseca

***Abstract*— Nanofiltration is currently applied in many industrial processes. The separation efficiency of nanofiltration systems is related to complex phenomena occurring at membrane surface and within the nanopores. The nature of these phenomena is still a subject of debate and there is a real need to better reproduce these phenomena through simple and accurate predictive models. In this paper, interfacial and dielectric properties of two commercial nanofiltration membranes are investigated with the modeling of the permeation of ions typically found in seawater. The membrane charge density was estimated using zeta potential measurements and the dielectric exclusion was represented by the Born model. The predictions of rejection and permeate flux were in good agreement with experimental results when the dielectric effect was considered, indicating that the calculation of membrane charge with zeta potential data is appropriate. Based on simulation results, dielectric constants inside nanopores were calculated and results show that the ion solvation model is appropriate for these membranes.**

***Index Terms*— Dielectric exclusion, Ionic rejection, Nanofiltration, Zeta potential.**

I. INTRODUCTION

Nanofiltration (NF) is a pressure-driven membrane separation process with characteristics between those of reverse osmosis and ultrafiltration and is currently applied in many industrial processes such as desalination [1]. The separation efficiency of nanofiltration systems is related to a complex mechanism including steric, dielectric and electrostatic partitioning effects between membrane and solutions [2], [3].

During the last two decades, the prediction of membrane performance has been a relevant area of research [1]. There is an increasing need for developing of model-based tools to design new membrane systems or to optimize existing membrane installations. These models should predict fluxes and rejections as a function of transmembrane pressure for a given membrane system. Also, they should be able to determine the membrane properties necessary to attain a desired retention and be a realistic predictive tool with a limited number of experiments [3], [4].

The most widely and successfully adopted NF predictive models are based on the extended Nernst – Planck (ENP) equation to describe the mass transfer across the membrane [3], [5], [6]. This model considers the three important mechanisms of ionic transport in membranes: (a) diffusion, (b) electromigration as a result of concentration and electrical potential gradients and (c) convection caused by the pressure difference across the membrane [7]. One of the most studied models is the Donnan-Steric Pore Model (DSPM) [8], [9]. This model describes the transport of ions in terms of an effective membrane thickness (Δx), a membrane charge density (X_d) and an effective pore radius (r_p) [5], [6], [8], [9]. It also takes into account the effects of hindrance to diffusion and convection within the pore and the equilibrium partitioning due to a combination of Donnan and sieving mechanisms at membrane / solution interfaces [6]. Although this model has been reported to successfully describe simple systems such as those constituted by organic molecules, it has not been very successful for multivalent cations. To improve the prediction capability, some modifications for DSPM model have been suggested by Bowen and Welfoot [9] such as the incorporation of dielectric constant variations between bulk and pore solutions, which has shown better prediction of divalent ions rejection. Bandini and Vezzani [10] proposed a more general model, called Donnan-Steric Pore Model & Dielectric Exclusion (DSPM&DE), which is basically an extension of the DSPM model, in which the primary effect of the DE is considered as the most relevant in determining ion partitioning, together with steric hindrance and Donnan equilibrium.

The membrane charge density is obtained by fitting rejection data in the DSPM and DSPM&DE models, being an empirical function related to the feed electrolyte concentration in terms of a Freundlich isotherm [10], [11]. This model is independent of the electrolyte type and does not consider any pH effect. It has been demonstrated to be appropriate in the case of single salts and multicomponent mixtures for some membranes, but it failed in some other cases [2]. Hence, it has been suggested that the membrane charge density is related to zeta-potential data by measuring the streaming potential of nanofiltration membranes, considering the influence of the ionic strength and pH. Other possibility is to develop physico-chemical models to describe the mechanism of charge formation, considering dissociations of functional groups [2], [12].

In this study, a model based on the DSPM models equations is used to predict the rejection of various ions

Marcela Costa Ferreira, School of Chemistry, Federal University of Rio de Janeiro, Rio de Janeiro, Brazil.
João Victor Nicolini, Chemical Engineering Program / COPPE, Federal University of Rio de Janeiro, Rio de Janeiro, Brazil.
Heloísa L. S. Fernandes, Chemical Engineering Department, School of Chemistry, Federal University of Rio de Janeiro, Rio de Janeiro, Brazil.
Fabiana Valéria da Fonseca, Inorganic Processes Department, School of Chemistry, Federal University of Rio de Janeiro, Rio de Janeiro, Brazil.

typically present in the seawater permeating through two different nanofiltration membranes. Zeta potential is incorporated in the model to estimate the membrane effective charge density for each salt solution studied. In the model the osmotic effect is considered by using the van't Hoff equation, while the dielectric exclusion is expressed in terms of the solvation energy barrier. The Born term and a variation of viscosity within the pore are also taken into account. The dielectric constant inside the pore (ε_p) is adjusted experimentally and the applicability of the single layer oriented molecules as the dominant dielectric exclusion mechanism is evaluated for both membranes. Finally, the simulation results using the DSPM-based models considering and not considering the dielectric exclusion mechanism are discussed and compared to the experimental data in order to validate the modified models for single salts solutions.

II. THEORY

A. *Transport Equations*

The Donnan-Steric Pore Model (DSPM), originally developed by Bowen *et al.* [8], describes the ionic transport across a membrane by the extended Nerst-Planck equation (ENP) [9]. Steric effects are caused by the difference between membrane pore radius and the ion Stokes radius, while electrical (Donnan) effect is the result of charge distribution in the membrane and in bulk solution. The combined effect determines the selective ions transport trough the membrane.

The ionic transport involves convection, diffusion and electric forces resulting in an ionic flux j_i through the membrane that is represented by ENP [9]:

$$j_i = K_{i,c} c_i U - \frac{c_i D_{i,\infty} K_{i,d}}{RT} \frac{d\mu_i}{dx} \tag{1}$$

where $K_{i,c}$ and $K_{i,d}$ are the hindrance factors for convection and diffusion of ion i, respectively, $D_{i,\infty}$ is the bulk diffusion coefficient of ion i ($m^2 s^{-1}$), μ_i is the electrochemical potential of ion i (J mol^{-1}), R is the universal gas constant (J mol^{-1} K^{-1}) and T is the temperature (K).

The pressure difference between both membrane sides causes a solvent velocity U inside the pore, which can be defined by the Hagen-Poiseuille equation (2). This assumption was validated elsewhere [9], [13].

$$U = r_p^{\,2} \Delta P_e / (8\eta \Delta x) \tag{2}$$

where ΔP_e is the effective pressure (Nm^{-2}) and η is the solvent viscosity (Nsm^{-2}).

The ENP equation is different from the Nerst-Planck equation because it considers hindrance factors that are important to correct the convective and diffusive transport for a solute confined in a pore [13]. The values of hindrance factors depend on the ratio of ionic Stokes radius to membrane pore radius, named λ_i and defined by (3), where r_i is the Stokes radius. Expressions for the calculation of hindrance factors were proposed by Bowen and Mohammad and are represented by (4) and (5) for $0 < \lambda i < 0.8$ [14].

$$\lambda_i = r_i / r_p \tag{3}$$

$$K_{i,c} = (1 + 2\lambda_i - \lambda_i^{\,2}) \times (1 + 0.054\lambda_i - 0.988\lambda_i^{\,2} + 0.441\lambda_i^{\,3}) \tag{4}$$

$$K_{i,d} = 1 - 2.3\lambda_i + 1.154\lambda_i^{\,2} + 0.224\lambda_i^{\,3} \tag{5}$$

The mass transfer is steady state, so that the mass accumulation rate is null. Thus the molar fluxes through boundaries must be equal to fluxes inside membrane [15]. The ionic flux of component i correlates the molar flux of component i at permeate ($C_{i,p}$) to solvent average velocity inside membrane [6], [9], [13], [16]:

$$j_i = C_{i,p} U \tag{6}$$

Substituting (2) and (6) into (1) yields the concentration gradient within the pore:

$$\frac{dc_i}{dx} = \frac{U}{D_{i,p}} \left[\left(K_{i,c} - \frac{D_{i,p}}{RT} V_i \frac{8\eta}{r_p^{\,2}} \right) c_i - C_{i,p} \right] - \frac{z_i c_i}{RT} F \frac{d\psi}{dx} \tag{7}$$

where c_i is the concentration within the pore (mol m^{-3}), D_{ip} is the pore diffusion coefficient ($m^2 s^{-1}$), V_i is the partial molar volume of i, z_i is the valence of ion i, F is the Faraday constant (96487 C mol^{-1}), ψ is the electrical potential within the pore (V) and $C_{i,f}$ and $C_{i,p}$ are the measured solute concentration in the feed and permeate sides, respectively.

The electroneutrality conditions at feed side, inside membrane pore and at permeate side are respectively:

$$\sum_{i=1}^{n} z_i C_{i,f} = 0 \tag{8}$$

$$\sum_{i=1}^{n} z_i c_i = -X_d \tag{9}$$

$$\sum_{i=1}^{n} z_i C_{i,p} = 0 \tag{10}$$

Differentiation of (9) with respect to x and multiplication of (7) by z_i and summation over all ions give (11), which describes the potential gradient [9]:

$$\frac{d\psi}{dx} = \frac{\sum_{i=1}^{n} \frac{z_i U}{D_{i,p}} \left[\left(K_{i,c} - \frac{D_{i,p}}{RT} V_i \frac{8\eta}{r_p^{\,2}} \right) c_i - C_{i,p} \right]}{F / (RT) \sum_{i=1}^{n} z_i^{\,2} c_i} \tag{11}$$

The Donnan equilibrium theory relates the electrochemical potential in the bulk feed solution to that within the pores [9] generating a difference in ions distribution at both membrane sides. The simultaneous contribution of Donnan and steric effects is usually represented by Donnan-Steric partitioning equation at feed and permeate sides, where $\Delta\psi_D(0)$ and $\Delta\psi_D(\Delta x)$ are the Donnan potential (V) at feed and permeate interfaces, respectively [9]:

$$\frac{\gamma_i c_i(0)}{\gamma_i{}^0 C_{i,f}} = \Phi_i \exp\left(-\frac{z_i F}{RT}\Delta\psi_D(0)\right) \quad (12)$$

$$\frac{\gamma_i c_i(\Delta x)}{\gamma_i{}^0 C_{i,p}} = \Phi_i \exp\left(-\frac{z_i F}{RT}\Delta\psi_D(\Delta x)\right) \quad (13)$$

where γ_i and $\gamma_i{}^0$ are the activity coefficient within the pore and in the bulk and $c_i(0)$ and $c_i(\Delta x)$ are the concentration of ion i at pore entrance and outlet, respectively, in mol m^{-3}.

Steric partition coefficient Φ_i is defined as the relation between solute concentration at bulk solution and at membrane pore and can be related to the parameter λ_i, defined in Eq. (14):

$$\Phi_i = (1-\lambda_i)^2 \quad (14)$$

The dielectric exclusion is mainly attributed to alterations in the solvent dielectric constant due to the confinement of water molecules within the pore. The effect known as Born effect corresponds to the variation of solvation energy when an ion is transferred from the bulk solution to the membrane pores. When the dielectric constant of the solution confined inside the pores is lower than that of the bulk solution, the excess solvation energy is positive and the ions are rejected by the membrane pores [9], [17].

This phenomenon has been represented in different ways. Bowen & Welfoot [9] have considered that the orientation of the water molecules at pore walls would lead to a reduction in dielectric constant, creating an energy barrier to solvation of ions into the pores which would increase salt rejection.

The DSPM-DE model [10] considers a dielectric exclusion term which is attributed to the interaction of the ion with the electrical charges, induced by the ion, at interface between materials of different dielectric constants (the membrane matrix and the solvent). These induced charges are called "image charges" [18]. However, this consideration was not included in this work since the small radius of NF pores makes the pore solvent dielectric approach that of membrane, reducing the effect of image forces while increasing the solvation energy barrier [9].

The consideration of dielectric exclusion due to a single layer of ordered water molecules was validated by Oatley *et al.* [19] for Desal-5-DK NF membrane and was included in the model as a solvation energy term which multiplies the right-hand side of (12) and (13). This gives (15) and (16) [9]:

$$\frac{\gamma_i c_i(0)}{\gamma_i{}^0 C_{i,f}} = \Phi_i \exp\left(-\frac{z_i F}{RT}\Delta\psi_D(0)\right)\exp\left(-\frac{\Delta W_i}{kT}\right) \quad (15)$$

$$\frac{\gamma_i c_i(\Delta x)}{\gamma_i{}^0 C_{i,p}} = \Phi_i \exp\left(-\frac{z_i F}{RT}\Delta\psi_D(\Delta x)\right)\exp\left(-\frac{\Delta W_i}{kT}\right) \quad (16)$$

The solvation energy barrier ΔW_i (J) is calculated from the Born model [9]:

$$\Delta W_i = \frac{z_i{}^2 e^2}{8\pi\varepsilon_0 r_i}\left(\frac{1}{\varepsilon_p}-\frac{1}{\varepsilon_b}\right) \quad (17)$$

The variation of the pore dielectric constant ε_p with pore size is estimated as follows [9]:

$$\varepsilon_p = 80 - 2(80-\varepsilon^*)\left(\frac{d}{r_p}\right) + (80-\varepsilon^*)\left(\frac{d}{r_p}\right)^2 \quad (18)$$

This equation was developed with geometrical arguments and taking bulk dielectric constant to be ε_b = 80 (water dielectric constant at 25°C). The dielectric constant of the layer of oriented water molecules ε^* shall be determined experimentally.

B. Membrane Charge Density

When a membrane is in contact with an aqueous electrolytic solution, it acquires an electric charge by many possible mechanisms such as dissociation of functional groups and adsorption of ions from solution. Thus membrane charges are influenced by the type and the concentration of ionic species in an electrolytic solution. Those surface charges have an influence on the distribution of ions in the solution due to the requirement of the electroneutrality of the system so that there is an excess of counter-ions in the adjacent solution. This leads to the formation of an electric double layer [2], [20].

A potential difference is created between the surface and the solution due to the membrane charge. The electrical potential decreases towards the solution until electroneutrality is reached. The electric double layer thickness represented by Debye length λ_D (m) is defined as follows:

$$\lambda_D = \sqrt{(RT\varepsilon_0\varepsilon_b)/(2F^2 I)} \quad (19)$$

where ε_0 is the permittivity of free space (8.85419 x 10^{-12} C^2 J^{-1} m^{-1}) and I is the ionic strength (mol m^{-3}) defined by:

$$I = 0.5\sum_i^n z_i{}^2 C_i \quad (20)$$

Membrane charge of polymeric membranes is generally negative at high pH values (above isoelectric points), is neutral at around pH 3 - 4 and switches to positive at low pH values (below isoelectric points). Furthermore the isoelectric points depend on the electrolyte concentration and the anions adsorption is prevalent on the membrane, since they show lower hydration radii than cations [2].

C. Osmotic Pressure Difference

The effective pressure difference ΔP_e is defined as the difference between the applied pressure ΔP and the osmotic pressure difference $\Delta\pi$:

$$\Delta P_e = \Delta P - \Delta\pi \quad (21)$$

The osmotic pressure difference $\Delta\pi$ is calculated considering the feed and permeates concentrations and can be estimated with the van't Hoff relation at low concentrations [15]:

$$\Delta\pi = RT\sum\left(C_{i,f} - C_{i,p}\right) \quad (22)$$

Other models have been proven to successfully predict the osmotic pressure, as the Pitzer equation, which was found to

predict the osmotic pressure within experimental error from dilute solutions up to an ionic strength pf 6 M. However, the Pitzer equation requires many salt parameters that many times are unavailable [5]. The van't Hoff equation is simpler and meets the requirement of having a predictive model with less dependence of experimental data.

The osmotic pressure difference is considered in the Hagen-Poiseuille equation to correlate the permeate flux with the applied pressure (23) [9]. This equation was used to evaluate the effectiveness of the van't Hoff relation to predict the experimental permeate flux.

$$j_v = \frac{r_p^{\,2}}{8\eta}\left(\frac{\Delta P - \Delta\pi}{\Delta x}\right) \tag{23}$$

III. Methodology

A. Membranes and Feed Solution

The membranes considered in this work were NF90 (Dow FilmTech) and NP030 (Microdyn-Nadir). The main characteristics of these membranes are shown in Table I.

Table I. Summary of NF90 and NP030 membranes characteristics

	NF90	**NP030**
Supplier	Dow FilmTec	Microdyn-Nadir
Material of skin layer[a]	Polyamide	Polyethersulfone
Max. temperature, °C[a]	45	95
Pore radius, nm	0.55[b]	0.93[b]
pH range[a]	3-9	0–14

[a]According to membranes supplier; [b] [5]; c [21]

In order to investigate the model adequacy for the NF90 polyamide membrane and for the NP030 polyethersulfone membrane and to assess differences in exclusion mechanisms between them, theoretical ion rejections of diluted single salts solutions typically present in seawater (NaCl, $MgSO_4$, $CaSO_4$ and Na_2SO_4) permeating through the NF90 and NP030 nanofiltration membranes were compared to the experimental results of Nicolini *et al*. [22]. The same experimental conditions were used in the simulations. The feed concentration, pH and zeta potential measurements for each salt solution are showed in Table II.

Table II. Permeation conditions for NF90 and NP030 membranes

Salts	**C_f (mol L^{-1})**	**pH**	**NF90 zeta potential (mV)**	**NP030 zeta potential (mV)**
NaCl	0.025	5.83	-33.06	-47.73
Na_2SO_4	0.025	6.22	-58.37	-23.06
$MgSO_4$	0.025	7.52	-27.25	-22.45
$CaSO_4$	0.025	5.83	-22.02	-25.89

The experimental performance of the nanofiltration membranes was evaluated using a membrane filtration set up described in [22]. The system was equipped with a feed tank (10 L) where the feed solution was kept at constant temperature (23ºC) by using a thermostatic bath. Feed solution was circulated through the membrane cell in preset flow rates and operation pressures, adjusted by flowmeter and a needle valve, respectively. The tests were performed in recirculation mode to keep feed concentration approximately constant.

A flatsheet membrane with an effective filtration surface of 0.0028 m^2 was used. Membranes were cut into circular pieces and then soaked overnight in ultra-pure deionized water. Afterwards, they were compacted at maximum operation pressure with ultrapure water or electrolyte solution until constant permeate flow. Membranes permeabilities were determined with ultra-pure water, at a cross-flow rate of 40 $L.h^{-1}$, varying applied pressure from 5 to 20 bar.

The effective membrane thickness, Δx, was directly obtained from the permeability of pure water (P_m) based on (24):

$$\Delta x = \frac{r_p^{\,2}}{8\eta P_m} \tag{24}$$

Zeta potential values showed in Table II were determined by Nicolini *et al*. [22] by tangential streaming potential measurements with an electrokinetic analyzer (SurPASS, Anton Paar) with a clamping cell. For each measurement, membrane samples of 55 mm x 25 mm were mounted opposite each other and separated with a spacer. The flow of an electrolyte solution through the channel under pressure generated a streaming potential, which was used to calculate the zeta potential with the Fairbrother-Mastin equation, (25) [23]:

$$\frac{\Delta\varphi}{\Delta P} = \zeta\,\frac{\varepsilon_0\varepsilon_r}{\eta_0\lambda_0}\left(\frac{\lambda_h R_h}{R}\right) \tag{25}$$

where ζ is the zeta potential (V), $\Delta\varphi$ is the measured streaming potential in the flow cell (V), ε_r is the relative dielectric constant of the electrolyte solution, λ_0 is the bulk conductivity of the circulating electrolyte (mS.m-1), η_0 is the bulk solvent viscosity (N.s m^{-2}), R_h and R are the measured electrical resistances (mV A^{-1}) across the flow channel filled with the saline reference solution and with the electrolyte solution, respectively.

B. Concentration Polarization

Rejections observed during the experiments are defined by observed rejection (R_{obs}):

$$R_{obs} = 1 - \frac{C_p}{C_f} \tag{26}$$

However, in the presence of concentration polarization, the actual concentration at the membrane entrance is the wall concentration (C_w), which is higher than the feed concentration (C_f). As a result, the real rejection of a solute (R_{real}) is higher than the observed rejection and is defined as follows:

$$R_{real} = 1 - \frac{C_p}{C_w} \tag{27}$$

The wall concentration can be correlated to the feed concentration by (28):

$$\frac{C_w - C_p}{C_f - C_p} = \exp\left(\frac{j_v}{k_c}\right) \tag{28}$$

where j_v is the volumetric flux through the membrane and k_c is the mass transfer coefficient in the polarized layer.

Many works that employed cross-flow modules in the permeation experiments in the laboratory scales reported low

or negligible concentration polarization [2], [14]. In the present work, the mass transfer coefficient for the laminar cross-flow cell was calculated with (29) [24]. The real rejections will be used for comparison with calculated rejections.

$$Sh = \frac{k_c d_h}{D_\infty} = 1.85 \mathrm{Re}^{0.33} Sc^{0.33} (d_h / L)^{0.33} \quad (29)$$

where d_h is the hydraulic diameter (m), L is the channel length (m), Re is the Reynolds number, Sc is the Schmidt number and Sh is the Sherwood number.

C. Model Description

Fig.1 illustrates the algorithm developed in this work for the simulation of the ion rejections using DSPM-based models. This flowchart represents the process pathway to predict the rejections and fluxes of salts solutions. The routine was implemented in the software Scilab and simulations results were compared to real experimental data in order to evaluate predictability of this model.

The following assumptions are usually considered in unidimensional models [13] and were also considered in this work: (1) concentration gradient is considered only along the membrane thickness Δx; (2) the electroneutrality condition must be fulfilled in the feed solution, membrane and permeate; (3) ion partitioning between membrane and solution is determined by Donnan equilibrium, steric effects and dielectric effects; (4) charge density is uniform along the membrane and (5) solute and solvent transport take place in cylindrical pores of known effective radius r_p.

The first step for solving the models equations involves an initial knowledge of membrane, solvent and ions parameters as well as operating conditions like temperature and pressure. Resolution involves an iterative step as ions concentration profile inside membrane depends on permeate concentration due to boundary conditions, the value of which is not known.

Water properties depend on temperature (T) and salinity (s). Equation (30) indicates the correlation [25] used in this work to estimate water viscosity in the bulk solution.

$$\eta = 1.234 \times 10^{-6} \exp\left(0.00212s + \frac{1965}{T}\right) \quad (30)$$

The properties of each of the ions involved in this study are summarized in Table III [5], [9]. These values were incorporated in the DSPM-based models.

Once water, ions and membrane properties information are known, transport model parameters can be determined using equations shown previously in this work.

Ions concentrations inside membrane pore entrance, $c_i(0)$, can be calculated from feed concentrations, $C_{i,f}$, with partitioning equation due to Donnan equilibrium and steric effects. Ions concentrations are related to each other by electroneutrality.

An initial guess of permeate concentration, $C_{i,p}$, is necessary to solve the concentration profile inside the pore, represented by ENP equation. Thus ions concentrations inside membrane pore exit, $c_i(\Delta x)$, can be determined. As $c_i(\Delta x)$ is also in equilibrium with $C_{i,p}$, permeate concentration can be estimated from partitioning. This iteration procedure is repeated until convergence constraint is reached. At this point, it is possible to calculate the rejections and compare with experimental data.

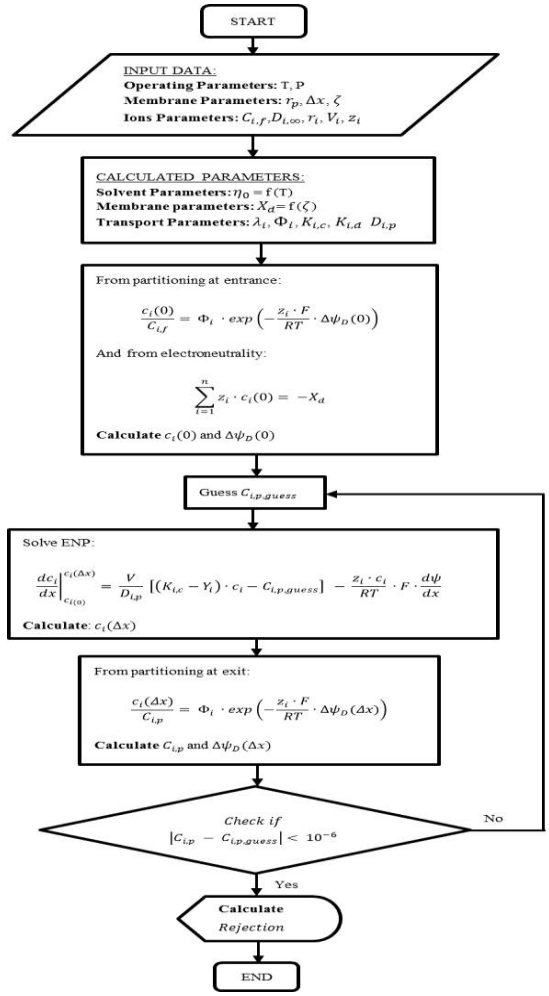

Fig. 1. Algorithm developed for the solution of models

Table III. Stokes radius, diffusivities and partial molar volumes of ions [5, 9]

Ions	r_i (nm)	$D_{i\infty}$ (10^{-9} m^2 s^{-1})	V_i (cm^3 mol^{-1})
Na^+	0.184	1.333	-1.20
Ca^{2+}	0.310	0.791	-18.04
Mg^{2+}	0.348	0.720	-21.57
Cl^-	0.121	2.031	17.82
SO_4^{2-}	0.231	1.062	14.18

The effective charge density model used in this work was determined by taking into account the solution ionic force, pH and zeta potential data. This model was chosen because it considers the pH information that has an important role in membrane charge formation, which is not taken into account in the rejection fitting models at different concentrations. This chosen model also depends less on experimental data and adjusting parameters than those which consider functional groups dissociation and ion adsorption terms.

In this model it is assumed that the effective surface charge density of the membrane is similar to the surface charge density at the shear plane (σ_s), which is calculated using the simplified Gouy-Chapmann equation [20]:

$$\sigma_s = \frac{\varepsilon_0 \varepsilon_b \zeta}{\lambda_D} \quad (31)$$

The membrane effective surface charge density can then be estimated using the zeta potential values. Assuming that the membrane surface charge is uniformly distributed in the

cylindrical pore, it is converted to concentration units by [12]:

$$X_d = (2\sigma_s)/(r_p F) \quad (32)$$

The zeta potential data obtained by measurements were used as input parameters to calculate membrane effective charge density. The simulations were carried on in the same conditions of experiments and the results were compared to investigate model accuracy.

IV. Results and Discussion

A. Determination of Real Rejections

The real rejections of salts were calculated based on the experimental observed rejections considering of the concentration polarization phenomena with (28). The results are presented in Table IV for maximum and minimum experimental pressures.

Table IV. Comparison of real and observed rejections for NF90 and NP030 membranes

Salts	ΔP (bar)	NF90			NP030		
		R_{obs} %	R_{real} %	ΔR %	R_{obs} %	R_{real} %	ΔR %
NaCl	20	0.940	0.961	2.1	0.299	0.326	2.8
	5	0.932	0.937	0.5	0.244	0.250	0.6
$MgSO_4$	20	0.988	0.993	0.5	0.637	0.683	4.7
	5	0.989	0.990	0.1	0.550	0.560	1.0
$CaSO_4$	20	0.990	0.995	0.5	0.695	0.733	3.9
	5	0.995	0.996	0.1	0.607	0.618	1.1
Na_2SO_4	20	0.993	0.996	0.2	0.787	0.812	2.5
	5	0.992	0.993	0.1	0.806	0.812	0.6

It can be noted form Table IV that the effect of concentration polarization decreases with decreasing membrane flux, as expected, for both membranes and all salt solutions. These results also show that the concentration polarization was low for the studied conditions. The maximum deviations from real to observed rejections were found to be 2.1% for NF90 membrane and 4.7% for NP030.

B. Permeate Flux Behavior

The pure water permeability of NF90 and NP030 membranes was 4.69 $Lh^{-1}m^{-2}bar^{-1}$ and 1.53 $Lh^{-1}m^{-2}bar^{-1}$ respectively. The effective membrane thickness was determined from (29) and found to be 0.49 µm and 9.9 µm for NF90 and NP030 membranes respectively. The difference between the thicknesses of the two membranes reflects the low permeability of NP030 membrane as compared to the NF90 membrane.

The calculated permeate fluxes were determined with (28). Fig. 2 shows the experimental and calculated permeate fluxes vs. applied pressure for each of the salts solutions and a comparison to the pure water flux through both membranes. The flux reduction is due to the osmotic effect which can be observed even at low concentrations. For all salts studied, there is a nearly linear relationship between calculated permeate fluxes and applied pressure, which was in agreement with the experimental data. Table V**Error! Reference source not found.** shows the comparison between calculated and experimental values on the basis of average deviation for all salts studied. These results show experimentally that the use of Hagen-Poiseuille equation defined in (2) is reasonable and confirm that the osmotic pressure can be well estimated using van't Hoff equation and should not be neglected.

C. Salt Rejections

Initial simulations were performed without considering the dielectric exclusion in order to investigate the importance of this phenomenon for each membrane. In these cases, pore dielectric constants ε_p were considered equal to bulk dielectric constant (ε_b = 80) for all salt solutions.

For the simulations using the model with the dielectric exclusion consideration, the magnitude of dielectric constant of ordered water layer, ε^*, was reassessed for each single salt solution using experimental data. The salts permeation was modeled with different dielectric constants of the oriented water layer lying between the two limiting values (ε^* = 6, when the water inside the pore is completely polarized, and ε^* = 80, when there is no polarization) and the optimum values which gave the best fit for each salt solution were found to be 33 ± 2 and 67 ± 5 for NF90 and NP030 membranes, respectively. Pore dielectric constants estimations were then calculated with Eq. (23) and are present in Table V.

Comparison between calculated and experimental permeate fluxes on the basis of average deviations (Dev.)

Salts	ΔP bar	NF90			NP030		
		$Jv_{,exp}$ (10-6 m/s)	$Jv_{,calc}$ (10-6 m/s)	Dev (%)	$Jv_{,exp}$ (10-6 m/s)	$Jv_{,calc}$ (10-6 m/s)	Dev. (%)
NaCl	20	24.73	24.64	0.37	7.07	6.95	1.64
	15	18.85	18.13	3.79	5.23	5.18	1.02
	10	12.37	11.61	6.15	3.53	3.44	2.51
	5	4.71	5.09	8.01	1.77	1.66	5.76
MgSO4	20	21.20	21.15	0.23	7.53	7.32	2.77
	15	17.67	15.47	12.44	5.78	5.43	6.09
	10	10.60	9.96	6.01	3.26	3.53	8.53
	5	4.71	4.31	8.54	1.50	1.65	10.08
CaSO4	20	24.31	23.21	4.54	7.07	6.81	3.69
	15	20.12	17.00	15.54	5.30	5.04	4.86
	10	12.60	10.93	13.28	3.53	3.28	7.19
	5	6.23	4.69	24.72	1.77	1.51	14.28
Na2SO4	20	21.20	19.85	6.38	7.07	6.52	7.77
	15	16.49	14.39	12.74	5.30	4.78	9.90
	10	10.60	8.96	15.51	3.53	2.99	15.52
	5	4.71	3.46	26.51	1.77	1.23	30.36

TableVI.

Fig. 3 shows the simulated rejections versus applied pressure for NaCl, Na_2SO_4, $CaSO_4$ and $MgSO_4$ solutions without and with the consideration of dielectric exclusion (no DE and with DE) for both NF90 and NP030 membranes. Regarding experimental data, Fig. 3 shows that although the solvent flux increases with pressure, the rejection remains practically constant for each salt solution. This suggests that ions fluxes also increase with pressure. The order of rejection

was Na_2SO_4 > $CaSO_4$ = $MgSO_4$ > NaCl for both membranes, which is a consequence of anionic electrostatic repulsion and the preferential attraction of divalent cations. Increased divalent cations concentration reduces the electrical exclusion of anions and, therefore, the saline rejection. NaCl salt presented the lowest rejection due to a less anionic repulsion for a monovalent ion and lower hydrated ionic radii.

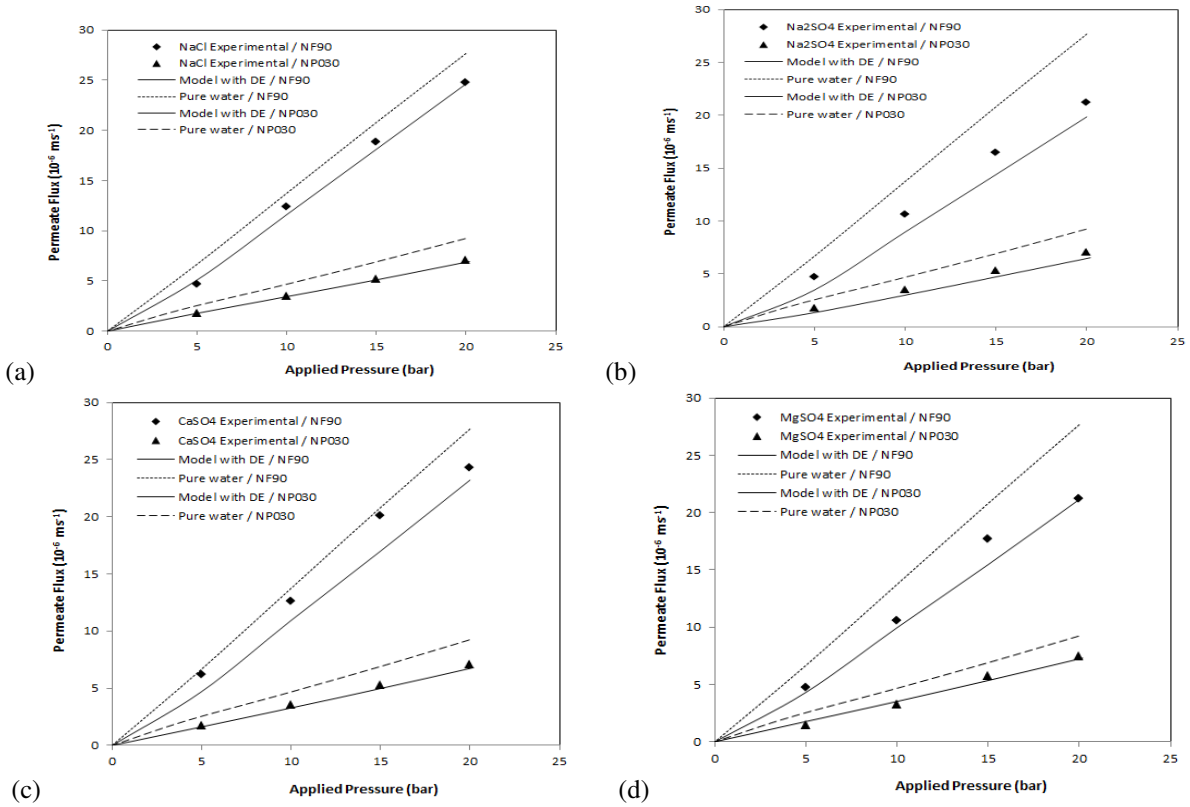

Fig. 2. Experimental and calculated permeate fluxes as a function of applied pressure for NF90 and NP030 membranes: (a) NaCl, (b) Na_2SO_4, (c) $CaSO_4$ and (d) $MgSO_4$

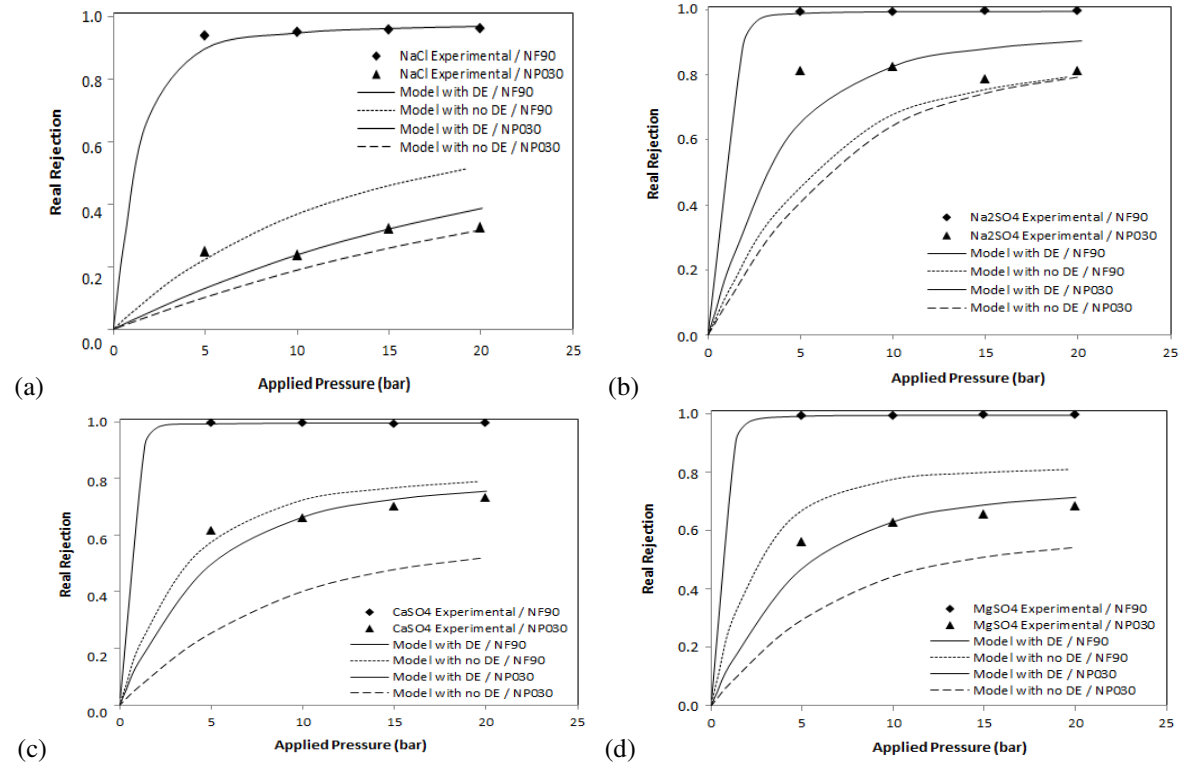

Fig. 3. Rejection of NF90 and NP030 membranes vs. applied pressure for different single salts solutions at 25 mmol.L^{-1}. The solid line represents rejection calculated with DE consideration and the dashed line represents rejection with no DE consideration: (a) NaCl, (b) Na_2SO_4, (c) $CaSO_4$ and (d) $MgSO_4$.

Table V. Comparison between calculated and experimental permeate fluxes on the basis of average deviations (Dev.)

Salts	ΔP bar	NF90			NP030		
		$J_{v,exp}$ (10^{-6} m/s)	$J_{v,calc}$ (10^{-6} m/s)	Dev (%)	$J_{v,exp}$ (10^{-6} m/s)	$J_{v,calc}$ (10^{-6} m/s)	Dev. (%)
NaCl	20	24.73	24.64	0.37	7.07	6.95	1.64
	15	18.85	18.13	3.79	5.23	5.18	1.02
	10	12.37	11.61	6.15	3.53	3.44	2.51
	5	4.71	5.09	8.01	1.77	1.66	5.76
$MgSO_4$	20	21.20	21.15	0.23	7.53	7.32	2.77
	15	17.67	15.47	12.44	5.78	5.43	6.09
	10	10.60	9.96	6.01	3.26	3.53	8.53
	5	4.71	4.31	8.54	1.50	1.65	10.08
$CaSO_4$	20	24.31	23.21	4.54	7.07	6.81	3.69
	15	20.12	17.00	15.54	5.30	5.04	4.86
	10	12.60	10.93	13.28	3.53	3.28	7.19
	5	6.23	4.69	24.72	1.77	1.51	14.28
Na_2SO_4	20	21.20	19.85	6.38	7.07	6.52	7.77
	15	16.49	14.39	12.74	5.30	4.78	9.90
	10	10.60	8.96	15.51	3.53	2.99	15.52
	5	4.71	3.46	26.51	1.77	1.23	30.36

Table VI. Dielectric constants from modeling of single salts solutions with NF90 and NP030 membranes

Salt	NF90		NP030	
	ε^*	ε_p	ε^*	ε_p
NaCl	30	42	73	76
Na_2SO_4	36	47	63	71
$MgSO_4$	33	44	67	73
$CaSO_4$	32	44	63	71

For all salts, the model with dielectric exclusion ($\varepsilon^* < 80$) predicted an increased rejection and led to a closer agreement between simulated and experimental data when compared to the DSPM model ($\varepsilon^* = 80$), indicating that the steric rejection and electrostatic partitioning alone are not capable of describing the rejection behavior. That emphasizes the importance of considering this effect in simulations.

The calculated values for ε^* (Table VI) are all in the range 30 to 36 for NF90 membrane and 63 to 73 for NP030 membrane. The resulting dielectric constants of the oriented layer were found to be 33 ± 2 and 67 ± 5 for NF90 and NP030 membranes, respectively. The result for NF90 membrane is in agreement with that report by [9] and [18] who obtained values of $\varepsilon^* = 34.5 \pm 2.5$, $\varepsilon^* = 35.5 \pm 1.5$ and $\varepsilon^* = 31$ for the NF270, NF99HF and Desal-5-DK membranes respectively, which are also a polyamide membranes. The dielectric constants for NP030 membrane are interesting results, as they are quite different from those reported in the literature for polyamide membranes. This divergence can be attributed, in part, both to the differences in the membranes active layer polymer, as NP030 is a polyethersulfone membrane and to the differences in pore size, as NF polyamide membranes have very narrow pores, up to twice as less than those of NP030. This suggests that the interaction between the solvent and the membrane and the reorganization of solvent molecules in polyethersulfone membranes is quite different from the polyamide ones and the dielectric exclusion mechanism is less important since the magnitude of pore dielectric constant remains closer to that of the bulk solution. The reduction in the dielectric constant for both membranes, even if in different magnitudes, also supports the hypothesis of a single layer of ordered water molecules with modified properties and suggests that the inclusion of the solvation energy term is suitable for describing the dielectric exclusion for both NF90 and NP030 membranes.

The deviations of average rejections predicted by the model from those obtained experimentally are present in Table VII.

Table VII. Comparison of simulated and experimental average rejections for NF90 and NP030 membranes

Salt	Average Deviation (%)	
	NF90	NP030
NaCl	1.51	16.77
Na_2SO_4	0.13	11.38
$CaSO_4$	0.19	6.91
$MgSO_4$	0.03	6.77

Good agreement between simulated and experimental results was observed with the model which considers the dielectric exclusion for both membranes. The accuracy obtained in the prediction of the experimental results using this consideration ranged from approximately 98.5% (for NaCl) to 100% (for $MgSO_4$) for NF90 and from approximately 83.2% (for NaCl) to 93.2% (for $MgSO_4$) for NP030 membranes. In the cases of $CaSO_4$ and $MgSO_4$ solutions for both membranes, deviations from the experimental rejections were less than in the cases of Na_2SO_4 and NaCl solutions. It should also be noted that the model was able to provide more accurate results for the polyamide membranes (NF90) than for polyethersulfone membranes (NP030). This is an information that engineers interested in predicting industrial performance of these commercial membranes should be aware of.

V. CONCLUSIONS

In the present work ion rejection by nanofiltration of four salt solutions was investigated by using a DSPM-based model with and without considering the dielectric exclusion mechanism. Zeta potential data was used to determine the membrane charge density, osmotic effects were considered through the introduction of van't Hoff equation in the model and pore dielectric constants were adjusted with experimental data. The aim of this study was to investigate the predictability of separation of the simple salts solutions of ions typically found in seawater by comparing the simulated rejection results with observed experimental data for two nanofiltration membranes, NF90 (polyamide membrane) and NP030 (polyethersulfone membrane). The concentration polarization was evaluated and the deviations between real and observed rejection were found to be low for both membranes. The results of predicted rejection and flux showed a good agreement when considering the dielectric effect by introducing the Born term in the model for both membranes, especially for NF90 membrane. However, when

this effect was not taken into account, the model underestimated the rejections for all salts solutions. This highlights the importance of considering the dielectric exclusion in the model and confirms that the determination of membrane charge density with zeta potential data can be considered. The dielectric constant of the oriented water layer was determined for each solution and found to be $\varepsilon^* = 33 \pm 2$ and $\varepsilon^* = 67 \pm 5$ for NF90 and NP030 membranes respectively, supporting that Born model is suitable to describe the dielectric exclusion for these membranes. The permeate flux behavior was also compared on the basis of average deviations which was considered low for each of the salts solutions at all pressures showing that the osmotic effect cannot be neglected in the model and that the van't Hoff equation can provide acceptable results.

REFERENCES

[1] D. L. Oatley-Radcliffe, S. R. Williams, M. S. Barrow, P. M. Williams, "Critical appraisal of current nanofiltration modelling strategies for seawater desalination and further insights on dielectric exclusion", *Desalination*, 343, 154-161, 2014.

[2] S. Bandini, "Modelling the mechanism of charge formation in NF membranes: Theory and application", *J. Membr. Sci.*, 264, 75–86, (2005).

[3] S. Bouranene, P. Fievet, A. Szymczyk, "Investigating nanofiltration of multi-ionic solutions using the steric, electric and dielectric exclusion model", *Chem. Eng. Sci.*, 64, 3789 – 379, 2009.

[4] J. Straatsma, G. Bargeman, H. C. van der Horst, J. A. Wesselingh, "Can nanofiltration be predicted by a model?", *J. Membr. Sci.*, 198, 273 – 284, 2002.

[5] A. W. Mohammad, N. Hilal, H. Al-Zoubi, N. A. Darwish, "Prediction of permeate fluxes and rejections of highly concentrated salts in nanofiltration membranes", *J. Membr. Sci.*, 289, 40-50, 2007.

[6] M. M. Zerafat, M. Shariati-Niassar, S. J. Hashemi, S. Sabbaghi, A. F. Ismail, T. Matsuura, "Mathematical modeling of nanofiltration for concentrated electrolyte solutions", *Desalination*, 320, 17-23, 2013.

[7] A. L. Ahmad, M. F. Chong, S. Bhatia, "Mathematical modeling and simulation of the multiple solutes system for nanofiltration process", *J. Membr. Sci.*, 253, 103-115, 2005.

[8] W. R. Bowen, A. W. Mohammad, N. Hilal, "Characterization of nanofiltration membranes for predictive purposes – use of salts, uncharged solutes and atomic force microscopy", *J. Membr. Sci.*, 126, 91-105, 1997.

[9] W. R. Bowen, J. S. Welfoot, "Modelling the performance of membrane nanofiltration—critical assessment and model development", *Chem. Eng. Sci.*, 57, 1121-1137, 2002.

[10] S. Bandini, D. Vezzani, "Nanoltration modeling: the role of dielectric exclusion in membrane characterization", *Chem. Eng. Sci.*, 58, 3303-3326, 2003.

[11] W. R. Bowen, H. Mukhtar, "Characterisation and prediction of separation performance of nanofiltration membranes", *J. Membr. Sci*., 112, 263-274,1996.

[12] G. Hagmeyer, R. Gimbel, "Modelling the rejection of nanofiltration membranes using zeta potential measurements", *Sep. Purif. Technol.*, 15,19–30, 1999.

[13] J.M. Gozálvez-Zafrilla, A. Santafé-Moros, "Nanofiltration Modeling Based on the Extended Nernst-Planck Equation under Different Physical Modes", Excerpt from the Proceedings of the COMSOL Conference 2008 Hannover.

[14] W. R. Bowen, A. W. Mohammad, "Diafiltration by Nanofiltration: Prediction and Optimisation", *A. I. Ch. E. J.*, 44, 1799-1812, 1998.

[15] T. R. Noordman, P. Vonk, V. H. J. T. Damen, R. Brul, S. H. Schaafsma, M. de Haas, J. A. Wesselingh, "Rejection of phosphates by a ZrO2 ultrafiltration membrane", *J. Membr. Sci.*, 135, 203-210, 1997.

[16] S. Déon, A. Escoda, P. Fievet, "A transport model considering charge adsorption inside pores to describe salts rejection by nanofiltration membranes", *Chem. Eng. Sci.*, 66, 2823–2832, 2011.

[17] F. Fadaei, V. Hoshyargar, S. Shirazian, S. N. Ashrafizadeh, "Mass transfer simulation of ion separation by nanofiltration considering electrical and dielectrical effects", *Desalination*, 284, 316-323, 2012.

[18] D. L. Oatley, L. Llenas, R. Pérez, P. M. Williams, X. Martínez-Lladó, M. Rovira, "Review of the dielectric properties of nanofiltration membranes and verification of the single oriented layer approximation", *Adv. Colloid Interface Sci.*, 173, 1-11, 2012.

[19] D. L. Oatley, L. Llenas, N. H. M. Aljohani, P. M. Williams, X. Martínez-Lladó, M. Rovira, J. Pablo, "Investigation of the dielectric properties of nanofiltration membranes", *Desalination*, 315, 100-106, 2013.

[20] J. Schaep, C. Vandecasteele, "Evaluating the charge of nanofiltration membranes", *J. Membr. Sci*., 188, 129–136, 2001.

[21] Z. Kovács, W. Samhaber, "Characterization of nanofiltration membranes with uncharged solutes", *Membrantechnika,* 12, 22–36, 2008.

[22] J. V. Nicolini, C. P. Borges, H. C. Ferraz, "Selective rejection of ions and correlation with surface properties of nanofiltration membranes", *Sep. Purif. Technol.*, 171, 238–247, 2016.

[23] A.E. Childress; M. Elimelech, "Effect of solution chemistry on the surface charge of polymeric reverse osmosis and nanofiltration membranes", *J. Memb. Sci.*, 119, 253–268, 1996.

[24] G. Schock, A. Miquel, "Mass transfer and pressure loss in spiral wound modules", *Desalination*, 64, 339–352, 1987.

[25] K. M. Sassi, I. M. Mujtaba, "Effective design of reverse osmosis based desalination process considering wide range of salinity and seawater temperature", *Desalination*, 306, 8-16, 2012.

Marcela Costa Ferreira holds a degree in Chemical Engineering from the Federal University of Rio de Janeiro, Brazil (2010), Master's degree in Sustainable Mobility Engineering – Specialization: Transport and Sustainable Development from the École Polytechnique, École des Ponts and École des Mines de Paris, France (2011) and Specialization in Upstream Process Engineering from the Federal University of Rio de Janeiro, Brazil (2014). She is currently a doctoral researcher at Federal University of Rio de Janeiro. She has experience in Chemical Engineering, with emphasis in Mathematical Modeling, Nanofiltration Processes, Process Engineering and Water Treatment.

João Victor Nicolini holds a degree in Chemical Engineering from the Faculdade de Aracruz, Brazil (2010), Master's degree (2013) and Doctorate (2017) in Chemical Engineering of the Federal University of Rio de Janeiro, Brazil. He is currently a postdoctoral researcher at the Chemical Engineering Program of the Federal University of Rio de Janeiro, Brazil. He has experience in Chemical Engineering, with emphasis in Interfacial Phenomena, Membrane Separation Processes and Advanced Oil Recovery.

Heloísa L. S. Fernandes holds a degree in Chemical Engineering from the Federal University of Rio de Janeiro, Brazil (2002), Doctorate (2007) and Post Doctorate (2009) in Chemical Engineering from the Federal University of Rio de Janeiro, Brazil. She is currently a professor at the School of Chemistry of the Federal University of Rio de Janeiro and participates as a professor of the Postgraduate Program in Chemical Processes and Biochemical Processes (EQ/UFRJ). She has experience in Chemical Engineering, with emphasis in Modeling of Chemical Processes.

Fabiana Valéria da Fonseca holds a degree in Chemical Engineering from the Federal University of Rio de Janeiro (2000), Master's degree (2003) and Doctorate (2008) in Technology of Chemical and Biochemical Processes of the Federal University of Rio de Janeiro. She is currently a professor at the School of Chemistry of the Federal University of Rio de Janeiro and participates as a permanent professor of the Postgraduate Program in Chemical Processes and Biochemical Processes (EQ/UFRJ) and the Environmental Engineering Program (UFRJ). She participates in the Integrated Nucleus of Reuse of Industrial Waters and Effluents (NIRAE / RJ). She has experience in Chemical Engineering, with emphasis in: Advanced Oxidative Processes, Treatment and Reuse of Water and Industrial Effluents, Removal of micropollutants in water, Chemical processes and Nanotechnology applied to water treatment